Available online at www.sciencedirect.com
ScienceDirect
Journal of the European Ceramic Society 32 (2012) 1389–1394
www.elsevier.com/locate/jeurceramsoc

Novel Na–Li–SiAlPON glasses prepared by melt synthesis using AlN

Abdessamad Kidari *, Michael. J. Pomeroy, Stuart Hampshire

Materials and Surface Science Institute, University of Limerick, Limerick, Ireland

Available online 26 January 2011

Abstract

Amorphous alumino–silicophosphate materials containing up to 1.70 wt.% nitrogen have been successfully prepared by aluminium nitride solution in Na–Li–Si–Al–P–O melts at 850 °C thus preventing phosphorus volatilisation. Although the solubility limit for nitrogen in these glasses was limited to 8.31 wt.%, the presence of nitrogen in the materials greatly increases their glass transition temperatures, suppresses the devitrification and has a significant effect on their melting behaviour. Comparative analysis of Raman spectra for the oxide and oxynitride glasses shows the substitution of P–O–P linkages by P=N–P linkages while tri-coordinated nitrogen bridges were not detected. The attendant increase in network connectivity arising from such a substitution is responsible for the increase in glass transition temperature when nitrogen substitutes for oxygen.

Keywords: Glass; Oxynitride; Alkali oxides; Spectroscopy; Thermal properties

1. Introduction

Anionic substitution in silicate[1–3] and phosphate[4–6] glasses has been widely explored over the past three decades. Nitrogen substitution for oxygen improves chemical, mechanical and thermal properties. This is because the substitution relies on the replacement of di-coordinated oxygen species by tri-coordinated nitrogen atoms,[1–4] and as nitrogen can theoretically bridge three tetrahedral centres, the network connectivity is increased.

Phosphorus oxynitrides are commonly prepared from the reaction of a phosphate melt containing modifier oxides and anhydrous ammonia at high temperatures (up to 800 °C).[4–6] While oxynitride glasses have been prepared in M–P–O–N, M–Si–O–N, M–Si–Al–O–N systems (where M is a modifier cation), glass preparation in systems containing aluminium and silicon and phosphorus have not been reported. This is probably, in part, due to the fact that the preparation of M–SiAlPON glasses by melting together nitrides and oxides would be complicated by the volatilisation of phosphorus under reducing conditions above 800 °C. Reactions (1) and (2) illustrate the reduction of phosphorus by silicon and aluminium nitrides:

$$\frac{1}{3}Si_3N_4 + \frac{2}{5}P_2O_5 \rightarrow \frac{2}{3}SiO_2 + \frac{2}{5}P_2^{\uparrow} + \frac{2}{3}N_2^{\uparrow} \quad \Delta G_{1073\,K} = -189\,kJ\ mol^{-1} \tag{1}$$

$$\frac{4}{3}AlN + \frac{2}{5}P_2O_5 \rightarrow \frac{2}{3}Al_2O_3 + \frac{2}{5}P_2^{\uparrow} + \frac{2}{3}N_2^{\uparrow} \quad \Delta G_{1073\,K} = -222\,kJ\ mol^{-1} \tag{2}$$

It is seen that there is a strong driving force for decomposition during these reactions even at the low firing temperature of 800 °C. Despite these unfavourable conditions, Rajaram and Day[6] succeeded in doping $NaPO_3$ glasses with aluminium nitride (AlN) without significant decomposition of the melt, and so it may be possible to prepare oxynitride glasses containing Si, Al and P by melt synthesis. This paper investigates the feasibility of preparation of M–SiAlPON glasses (M = Na and Li) with increasing nitrogen concentrations for constant cation ratios. In addition, it reports initial indications of structural changes in the glass on the basis of Raman spectral data.

2. Experimental procedure

2.1. Materials and processing

Two datum oxide compositions, $30Na_2O{:}20Li_2O{:}10SiO_2{:}30P_2O_5{:}10Al_2O_3$ and $30Na_2O{:}20Li_2O{:}5SiO_2{:}30P_2O_5{:}15Al_2O_3$ (in mol.%), prepared from $NH_4H_2PO_4$ (Fisher 99.35%), Na_2CO_3 (BDH 99%), Li_2CO_3 (Fisher 99%), Al_2O_3 (Sumitomo 99%) and SiO_2 (Fluka 99.8%) were specifically formulated to give rise to low liquidus temperatures. The dry mixed powders were fired in a platinum crucible for 30 min at 1250 °C (Car-

* Corresponding author.
E-mail addresses: abdessamad.kidari@gmail.com, abde.kidari@ul.ie (A. Kidari).

0955-2219/$ – see front matter © 2011 Elsevier Ltd. All rights reserved.
doi:10.1016/j.jeurceramsoc.2010.12.034

bolite CSF 1500), the melt was quenched between rectangular steel plates and the resulting glass frits milled and sieved down to 45 μm.

Additional aluminium deficient glasses were prepared for each datum composition (see Table 1). This deficiency in Al_2O_3 was introduced in order to account for the aluminium otherwise introduced by aluminium nitride so that addition of the appropriate amount of AlN yielded glasses with a constant cation ratio and only oxygen and nitrogen contents were changed. The drawback to this method is that the maximum theoretical nitrogen concentration that can be batched will be limited by the aluminium content in the datum composition.

The oxynitride batches made from the Al-deficient oxides and AlN were dry mixed and 3 g batches were fired in pyrolytic boron nitride crucibles (Almath Crucibles Ltd.) at 850 °C for 150 min under flowing nitrogen atmosphere (200 ml min^{-1}) then quenched under air at room temperature.

2.2. Characterisation

The powdered materials were pressed into 32 mm disks with ethyl cellulose and their amorphicity checked using X-ray diffraction (Philips X'pert PRO MPD PW3050). Thermal traces were recorded using differential thermal analysis (DTA Stanton Redcroft STA 1640) on 30 mg of the samples using a heating rate of 10 °C min^{-1} under a constant flow of 80 ml min^{-1} of nitrogen.

The total nitrogen content was determined by alkaline digestion in molten KOH at 450 °C of 25 mg of the sample thus leading to the release of ammonia.[7] Nitrogen released as ammonia was neutralised in a 0.003 M H_2SO_4 solution and back titrated with a standardised NaOH solution.

$$2N^{3-} + 6KOH \rightarrow 2NH_3 + 3K_2O + 3O^{2-} \quad (3)$$

Specimens were subjected to Raman analysis (Labram DILOR XY) with spectra collected using a 514.5 nm green laser source (He–Ne 20 mW). A grating number of 1800 was used in association with a Peltier cooled CCD detector and the system was coupled to a confocal microscope (Olympus BX40 50× objective).

3. Results and discussion

3.1. Glass formation and differential thermal analysis

Table 1 summarises the characteristics of the materials after firing, their measured nitrogen contents and their glass transition temperatures. The fired materials contained few bubbles evenly distributed in their bulk and their colour changed from light grey for 4.1 wt.% N to dark grey for the samples batched with 8.4 wt.% N. No visible signs of phosphorus decomposition (yellow coloration and/or PH_3 gas release) could be detected during and after firing and the weight losses measured on the samples, shown in Table 1, confirm the stability of the melt.

It is seen that for both alumina contents, amorphous oxynitrides were obtained with AlN additions of approximately 4.1 and 8.4 wt.% while for the higher AlN addition (≈12.6 wt.%), AlN reflections were observed showing that not all the added aluminium nitride had dissolved. Increases in the melting time, from 2.5 to 5 h, and in the firing temperature, from 850 to 900 °C, did not enhance the solubility of the nitride in the melt, thus confirming that the solubility limit for AlN was reached. The measured nitrogen contents of the amorphous materials indicate a solubility limit of ≈1.7 wt.% N (Table 1). These measured nitrogen levels were consistently below the nitrogen content calculated from the batch composition and Table 1 details the differences. In general the nitrogen retention was 55–60%. From the data presented, it is clear that novel Li–Na–Si–Al–P–O–N glasses can be prepared by the addition of AlN to low melting oxide glass precursors.

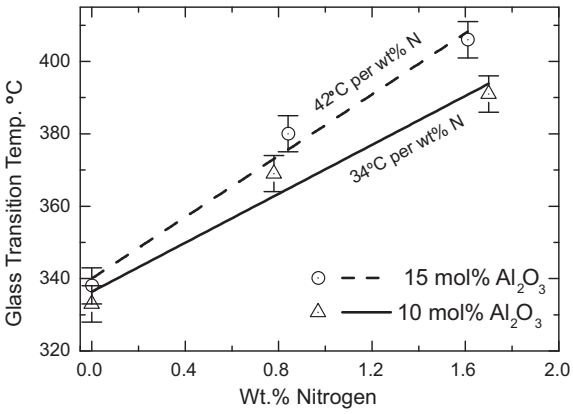

Fig. 1. Glass transition temperature dependency upon the nitrogen content of Na–Li–Si–Al–P–O–N glasses with 10 and 15 mol% Al_2O_3.

Differential thermal analysis traces for the oxide glasses and their respective oxynitrides are shown in Fig. 2. The glass transition region of the oxides is shifted toward higher temperatures in the nitrogen containing glasses. Table 1 and Fig. 1 detail the variation in T_g with nitrogen content for the two different glass compositions. It is seen that T_g increases monotonically with nitrogen at a rate of 34 °C and 42 °C per wt.% N for the glasses with 10 and 15 mol.% Al_2O_3, respectively (for clarity, the aluminium content of the oxynitrides is expressed in mol.% Al_2O_3). These gradients are much greater than for other oxynitride systems, ≈8 °C per wt.% N for Na–P–O–N and ≈18 °C per wt.% N for Ca–Si–Al–O–N glasses.[4,8]

The glass with 10 mol% Al_2O_3 exhibits two exothermic peaks of crystallisation at about 399 °C and 425 °C (see Fig. 2a), these are not detected on the DTA trace of the oxynitride glass containing 0.78 wt.% N while the oxynitride containing 1.70 wt.% N shows two exothermic features at about 446 and 552 °C the nature of which could not be established. For the glass with 15 mol% Al_2O_3, crystallisation peaks are visible at 378 and 398 °C (see Fig. 2b), for 0.84 wt.% N the oxide glass crystallisation peaks are not detected while a small exotherm appears at about 431 °C. Finally, the glass with 15 mol% Al_2O_3 shows a crystallisation peak at about 499 °C when the nitrogen content reaches 1.61 wt.%.

In the same Fig. 2a and b, it can be seen that sharp melting peaks occur at about 598 °C and 602 °C, for the glasses with 10

Table 1
Compositions and properties of Na–Li–Si–Al–P–O glasses doped with AlN.

Datum compositions (mol.%)[a]					AlN addition (wt.%)	X-ray analysis	Weight loss (%)	Batched N (wt.%)	Measured N (wt.%)	Tg (°C)
Na_2O	Li_2O	SiO_2	P_2O_5	Al_2O_3						
30	20	10	30	10	0.00	Amorphous	–	0.00	0.00	338
31.30	20.87	10.43	31.30	6.09	4.12	Amorphous	−0.06	1.41	0.78	380
32.73	21.82	10.91	32.73	1.82	8.32	Amorphous	−0.23	2.84	1.70	406
30	20	5	30	15	0.00	Amorphous	–	0.00	0.00	333
31.33	20.89	5.22	31.33	11.23	4.14	Amorphous	+0.02	1.41	0.84	369
32.79	21.86	5.46	32.79	7.10	8.37	Amorphous	−0.18	2.86	1.61	391
34.38	22.92	5.73	34.38	2.58	12.68	AlN[b]	–	4.31	–	–

[a] AlN additions yield compositions with identical cation ratios.
[b] Partly crystalline.

and 15 mol% Al_2O_3, respectively. When the nitrogen content reaches 0.78 wt.% the peak is sharp and when 1.70 wt.% N is attained, the intensity of the melting peak decreases significantly and shifts toward higher temperatures. In a similar manner, nitrogen substitution for oxygen in the glass with 15 mol.% Al_2O_3 up to 0.84 wt.% N leads to a decrease in the intensity of the melting peak located at 602 °C and when the nitrogen content reaches 1.61 wt%, this peak is not detected. Oxygen replacement by nitrogen also leads to a widening (toward higher temperatures) of the endothermic region located above 600 °C which indicates that the oxynitride materials melt over a wider temperature range.

From the above analyses it is clear that the replacement of oxygen by nitrogen affects the thermal characteristics of Na–Li–Si–Al–P glasses:

(i) The glass transition temperature increases monotonically with nitrogen.
(ii) For a nitrogen content of 0.78 and 0.84 wt.% in the glasses with 10 and 15 mol.% Al_2O_3, respectively, the driving force for crystal growth is significantly lower than in the oxide system.
(iii) For nitrogen contents of 1.61 and 1.70 wt.%, crystallisation peaks can be distinguished at temperatures well above those found for the nitrogen-free glasses and the extent of crystal growth is more limited in comparison to the oxides.
(iv) The main endothermic melting peak common to both oxide glasses is severely affected by nitrogen incorporation.

All these features indicate the development of greater network connectivities in the Li–Na–Si–Al–P–O–N oxynitride glasses. The replacement of di-coordinated oxygen by nitrogen, which can theoretically bridge up to three tetrahedral centres, increases the degree of crosslinking of the network; it is therefore understandable that these higher connectivities affect the temperature dependant properties and related phenomena. As the correlation between the changes in the thermal properties of Na–Li–Si–Al–P–O–N glasses with their nitrogen fraction have been established, in the following section, the relationship between structure and properties is explored by means of Raman spectroscopy.

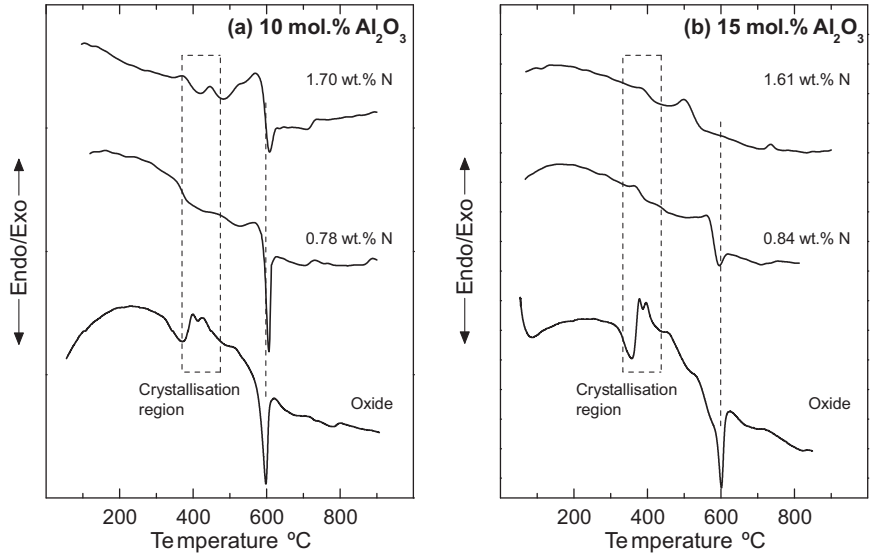

Fig. 2. DTA traces for the oxide and oxynitride glasses with (a) 10 mol% Al_2O_3, (b) 15 mol.% Al_2O_3.

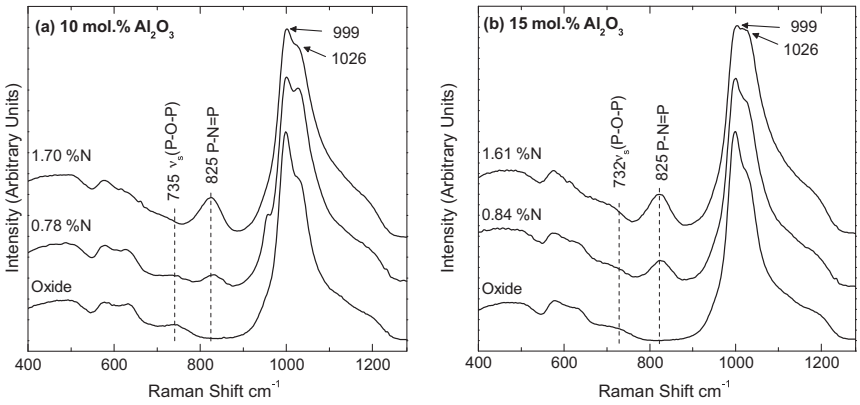

Fig. 3. Raman spectra of the oxides with (a) 10 and (b) 15 mol% Al_2O_3 and their respective oxynitrides.

3.2. Raman spectroscopy structural analysis

Fig. 3 shows Raman spectra for the amorphous oxide and oxynitride materials and Table 2 summarises the peak assignments used. Both oxide glasses (10 and 15 mol.% Al_2O_3) show Raman bands at approximately 400–540, 575, 630 and 735 cm^{-1} and there is broad composite peak over the 900–1250 cm^{-1} range. For the phosphate part of the glass network, the Raman data gives information on the n value in the Q^n expression typically associated with phosphate materials. The 735 cm^{-1} band originates from the stretching motion for P–O–P bridges in Q^1 pyrophosphate tetrahedra and the band at about 575 cm^{-1} and between 400 and 540 cm^{-1} from the symmetric stretching of phosphorus – non-bridging oxygen bonds (i.e. $P–O^-$ bonds) and O–P–O bending modes of Q^0 orthophosphate units, respectively.[9–11] The broad peak at the higher wavenumbers arises from phosphorus – non-bridging oxygen bonds associated with Q^1 species (1026 cm^{-1}).[9,10] The shoulders at about 1118 and 1186 cm^{-1} can be attributed to $P–O^-$ symmetric stretching in terminal Q^1 units and Q^2 phosphate tetrahedra, respectively, and there is a slight shoulder at about 950 cm^{-1} which can be attributed to symmetric stretching of P-NBO bonds in Q^0 orthophosphate tetrahedra; this mode overlaps with silicate structural motions giving rise to an intense peak at 999 wavenumbers.[9,12] While such overlaps due to Si and Al may arise, the significant P:Si and P:Al ratios in the compositions would tend to suggest that the majority of the Raman signature originates from the phosphate network. Since there is no visible contribution to the Raman signal from the motion of P–O–P bridges belonging to Q^2 phosphate chains (two bridging oxygen per tetrahedron found around 700 cm^{-1}), and based on the above description of the Raman spectra for the oxide glasses, it is apparent that the predominant Raman peaks arise for bonds associated with Q^0 and Q^1 tetrahedral phosphate species.

Table 2
Raman bands and peaks assignments.

Frequency (cm^{-1})	P-network assignments	Si-network assignments
400–450	O–P–O bending (Q^0)	
575	P–NBO_{sym} stretch (Q^0)	Si–O–Si bend (Q^3)
630		Si–O–Si bend (Q^2)
735	P–O–P_{sym} stretch (Q^1)	
825	P=N–P stretch	
950	$(PO_4)_{sym}$ stretch (Q^0)	Si–NBO stretch (Q^2)
999	–	
1026	$(PO_3)_{sym}$ stretch (Q^1)	
1118	P–O stretch terminal Q^1	Si–NBO stretch (Q^3)
1186	$(PO_3)_{sym}$ stretch (Q^2)	

In addition to this analysis from the Raman spectra of the phosphate network, it should be noted that silicate structures of Q^2 connectivity may be associated with the 999 cm^{-1} peak and Q^3 SiO_4 tetrahedra give rise to a Raman shift at 1100 cm^{-1} and may thus contribute to the intensity of this peak.[13–15] Raman peaks appear at 630 and 575 cm^{-1} corresponding to bending of Si–O–Si bonds (corner shared bridging oxygens) in Q^2 and Q^3 silicate structures.[13–15] The presence of aluminium in 6-fold coordination is also revealed by a Raman peak at about 630 cm^{-1}.[16] Thus, Q^0 and Q^1 structural units constitute the dominant phosphate tetrahedral structure and this would be expected from the highly modified oxide glass compositions.

Comparison of the Raman spectra for the two oxide glasses (Fig. 3a and b) indicates that the relative intensities of the 630 and 735 cm^{-1} bands decrease significantly when the Al_2O_3 is increased from 10 to 15 mol.%. The oxide glass containing 15 mol% Al_2O_3 thus has a lower concentration of P–O–P bridges due to their replacement by P–O–Al ones. The reduced silica content of the glass containing 15 mol.% Al_2O_3 also results in decreased numbers of Si–O–Si linkages. Both of these structural modifications depolymerise the glass network.

The substitution of oxygen by nitrogen gives rise to significant differences in the Raman response of the glasses. The most obvious change in the nature of the Raman information is the decreasing intensity of the P–O–P motion at 735 cm^{-1} and the development of a new Raman peak at 825 cm^{-1}, the intensity of which increases with nitrogen content (see Fig. 3a and b). The band at 825 cm^{-1} is assigned to P–N=P stretching[17] indicating that the substitution of oxygen by nitrogen results in anion exchange at bridging sites. This band is located 12 cm^{-1} above the value reported by Bunker et al.[17] (813 cm^{-1}) and its positions is not affected by the aluminium and silicon contents of the glass (825 cm^{-1} for 10 and 15 mol.% Al_2O_3). Since (i) the frequency of P–O–P bridges motion increases when the length of the phos-

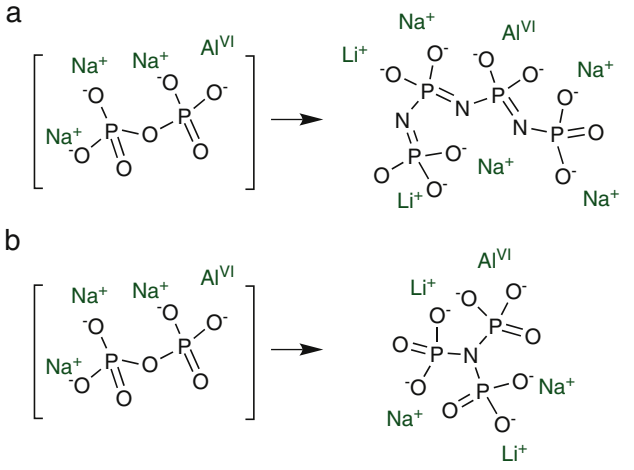

Fig. 4. Anionic strengthening of Q^1 pyrophosphate structures through (a) tri-coordinated nitrogen and (b) di-coordinated nitrogen linkages.

phate chain decreases[10], and (ii) as the glasses investigated by Bunker et al.[17] are metaphosphates of Q^2 connectivity where the P–O–P motion appear at 690 cm^{-1}, this frequency shift probably results from the formation of P=N–P bridges within shorter phosphate chains. The absence of any dependency of the P=N–P motion frequency on the silicon and aluminium contents is not clear; it might suggest that the affected tetrahedra are Si and Al-free but additional evidence is needed here.

The change in Raman signatures with nitrogen substitution level is effectively the same for the two different compositions (10 and 15 mol.% Al_2O_3). The relative intensity of the phosphorus – non-bridging oxygen peak at 575 cm^{-1} remains unchanged when nitrogen substitution occurs which is consistent with the work of Marchand et al.[18] and Boukbir et al.[19] who reported that the bonding between modifier ions and non-bridging oxygens is unaffected when nitrogen replaces oxygen in phosphorus oxynitride glasses. Furthermore, as it is also known that Al–O–P linkages are stable,[20] then only P–O–P bridges from Q^1 phosphate structures and double bonded terminal oxygens are potential substitution sites. The nitrogen substitution process induces an increase in intensity at 1026, 1118 and 1186 cm^{-1} compared to the oxide glasses. It is thought that this intensity increase results from an overall increase in network connectivity but no assumptions can be made at this stage because of strong overlap between Si and P species in these regions and the absence of spectral information that would fully demonstrates N/O substitution in SiO_4 tetrahedra.

The increase in network connectivity implied by the T_g data could stem from one or both of two mechanisms: (i) the replacement of P–O–P bonds by P–N=P bonds (i.e. di-coordinated nitrogen), thus removing P=O terminations and facilitating longer chain units as shown in Fig. 4a, (ii) the replacement of –O– linkages by –N< linkages shown in Fig. 4b (i.e. the replacement of di-coordinated oxygen by tri-coordinated nitrogen in the silicate and phosphate networks), thus linking three tetrahedral units and increasing the level of cross-linking in the glass.

Both mechanisms are accounted for by the nitridation of Si-free metaphosphate glasses[18] but, as stated above, there is direct evidence from the development of the band at 825 cm^{-1} to support the increase in network connectivity afforded by mechanism (i) and the Raman data only shows a declining peak at 630 cm^{-1} which is where –N< bridges in P–O–N systems have previously been observed.[17] Accordingly, there is no direct evidence for nitridation of the phosphate network according to mechanism (ii).

4. Conclusions

Amorphous Na–Li–Si–Al–P–O–N oxynitride materials containing up to 1.70 wt.% nitrogen can be prepared by the dissolution of AlN in precursor glasses, and to the authors' knowledge, this is the first reported successful synthesis of nitrogen-containing alumino–silicophosphate glasses. Glass transition temperatures for the oxynitride glasses increase with increasing nitrogen content and do so much more significantly than is the case for NaPON or CaSiAlON glasses while the tendency toward devitrification is suppressed. The increases in network connectivity, reflected by the increases in glass transition temperatures, arise as a result of the replacement of P–O–P bridges by P=N–P linkages, which remove P=O terminations, thus increasing, on average, the potential number of linkages between each phosphorus and the amorphous network. Current ongoing work focuses on 1D and MQ MAS-NMR structural analysis of these glasses in order to understand the exact effect by which nitrogen causes mechanical and thermal property values to change.

Acknowledgement

The authors wish to acknowledge financial support from Science Foundation Ireland under Grant No. 05/RFP/CHE0091.

References

1. Hampshire S, Pomeroy MJ. Oxynitrides glasses. *Int J Appl Ceram Technol* 2008;**5**(2):155–63.
2. Hampshire S, Drew RAL, Jack KH. Oxynitride glasses. *Phys Chem Glasses* 1985;**26**(5):182–6.
3. Sun EY, Becher PF, Hwang SL, Waters SB, Pharr GM, Tsui TY. Properties of silicon–aluminium–yttrium oxynitride glasses. *J Non-Cryst Solids* 1996;**208**:162–9.
4. Marchand R. Nitrogen containing phosphate glasses. *J Non-Cryst Solids* 1983;**56**(1–3):173–8.
5. Reidmeyer MR, Rajaram M, Day DE. Preparation of phosphorus oxynitride glasses. *J Non-Cryst Solids* 1986;**85**(1–2):186–203.
6. Rajaram M, Day DE. Cation effects in $NaPO_3$ glasses doped with metal nitrides and oxides. *J Am Ceram Soc* 1986;**69**(5):400–3.
7. Guyader J, Grekov FF, Marchand R, Lang J. New series of silicoapatites enriched with nitrogen. *Rev Chim Miner* 1978;**15**(5):431–8.
8. Sakka S, Kamiya H, Yoko T. Preparation and properties of Ca–Al–Si–O–N oxynitrides glasses. *J Non-Cryst Solids* 1983;**56**(1–3):147–55.
9. Brow RK. Review: the structure of simple phosphate glasses. *J Non-Cryst Solids* 2000;**263–264**:1–28.
10. Pemberton JE, Latifzadeh L. Raman spectroscopy of calcium phosphate glasses with varying CaO modifier concentrations. *Chem Mater* 1991;**3**(1):195–200.
11. Karakassides MA, Saranti A, Koutselas I. Preparation and structural study of binary phosphate glasses with high calcium and/or magnesium content. *J Non-Cryst Solids* 2004;**347**(1–3):69–79.

12. Brow RK, Tallant DR, Myers ST, Phifer CC. The short-range structure of zinc polyphosphate glass. *J Non-Cryst Solids* 1995;**191**(1–2):45–55.
13. McMillan P. Structural studies of silicate glasses and melts-applications and limitations of Raman spectroscopy. *Am Mineral* 1984;**69**(7–8):622–44.
14. Mysen BO, Virgo D, Kushiro I. The structural role of aluminum in silicate melts – a Raman spectroscopic study at 1 atmosphere. *Am Mineral* 1981;**66**(7–8):678–701.
15. McMillan P. A Raman spectroscopic study of glasses in the system CaO–MgO–SiO_2. *Am Mineral* 1984;**69**(7–8):645–59.
16. Belkébir A, Rocha J, Esculcas AP, Berthet P, Gilbert B, Gabelica Z, et al. Structural characterisation of glassy phases in the system Na_2O–Al_2O_3–P_2O_5 by MAS and solution NMR, EXAFS and vibrational spectroscopy. *Spectrochim Acta Part A* 1999;**55**(7–8):1323–36.
17. Bunker BC, Tallant DR, Balfe CA, Kirkpatrick RJ, Turner GL, Reidmeyer MR. Structure of phosphorus oxynitride glasses. *J Am Ceram Soc* 1987;**70**(9):675–81.
18. Marchand R, Agliz D, Boukbir L, Quemerais A. Characterization of nitrogen containing phosphate glasses by X-ray photoelectron spectroscopy. *J Non-Cryst Solids* 1988;**103**(1):35–44.
19. Boukbir L, Marchand R, Laurent Y, Chao ZJ, Parent C, Le Flem G. A structural investigation of phosphorus oxynitride glasses. *J Solid State Chem* 1990;**87**(2):423–9.
20. Benitez JJ, Diaz A, Laurent Y, Odriozola JA. Study of aluminophosphate oxynitride (AlPON) materials by X-ray photoelectron (XPS) and diffuse reflectance Fourrier transform IR spectroscopy (DRIFTS). *J Mater Chem* 1998;**8**(3):687–91.